Carbon *K*-shell excitation of gaseous and condensed cyclic hydrocarbons: C_3H_6, C_4H_8, C_5H_8, C_5H_{10}, C_6H_{10}, C_6H_{12}, and C_8H_8

A. P. Hitchcock, D. C. Newbury, and I. Ishii
Department of Chemistry, McMaster University, Hamilton, Canada L8S 4M1

J. Stöhr
IBM Almaden Research Center, San Jose, California 95120-6099

J. A. Horsley and R. D. Redwing
Corporate Research Science Laboratories, Exxon Research and Engineering Company, Annandale, New Jersey 08801

A. L. Johnson[a)]
MMRD, Lawrence-Berkeley Laboratory, Berkeley, California 94720

F. Sette
AT&T Bell Laboratories, Murray Hill, New Jersey 07974

(Received 9 May 1986; accepted 22 July 1986)

The carbon *K*-shell excitation spectra of gaseous cyclic hydrocarbons, both saturated (cyclopropane, cyclobutane, cyclopentane, cyclohexane) and unsaturated (cyclopentene, cyclohexene, and cyclooctatetraene), have been recorded by electron energy loss spectroscopy under dipole-dominated conditions. These are compared to the NEXAFS spectra of multilayers and monolayers of C_4H_8, C_5H_8, C_6H_{12}, and C_8H_8 on Pt(111). Multiple scattering $X\alpha$ calculations of the spectra of cyclopropane, cyclobutane, and cyclohexane are also reported. In most cases the gas and solid spectra are essentially the same indicating that intramolecular transitions dominate in the condensed phase. The NEXAFS polarization dependence of the condensed phases has assisted spectral assignments and the determination of the molecular orientation in the monolayer phase. In the saturated species a sharp feature about 3 eV below the carbon 1*s* ionization threshold is identified as a transition to a state of mixed Rydberg/valence character with the $\pi^*(CH_2)$ valence component dominating. Except for cyclopropane the positions of the main σ^* resonances correlate with the C–C bond lengths in a manner similar to that reported previously for noncyclic aliphatic molecules. In the spectra of monolayer C_6H_{12}, C_5H_8, and C_8H_8 spectral broadening and weak additional features are observed which are attributed to molecule–surface interactions.

I. INTRODUCTION

Over the last few years *K*-shell excitation studies by inner shell electron energy loss (ISEELS)[1] and near edge x-ray absorption fine structure (NEXAFS)[2–5] spectroscopies have proven to be particularly useful in examining the electronic structure of molecules containing the second row elements C, N, O, and F. Carbon containing molecules are of particular interest. Among the more significant recent discoveries is an empirical correlation between bond length and σ shape resonance position.[2] In addition to intramolecular bond length determination, the polarization dependence of NEXAFS spectra provides information on the *orientation* of molecules in the solid state and chemisorbed on surfaces.[3] The spectroscopic and structural information in the spectra of gas phase, solid, and chemisorbed molecules is best interpreted by combining these results. Gas phase spectra provide information which concern only *intra*molecular transitions. These can be compared to the solid and monolayer spectra to identify effects due to *inter*molecular or molecule–surface interactions. In a recent study of benzene and pyridine[4] the gas, solid, and monolayer spectra were found to be dominated by a common set of intramolecular resonances. This indicates that the *K*-shell excitations are predominantly intramolecular and that transitions to states based on intermolecular interactions are weak or absent.

The features observed in the *K*-shell spectra of free molecules are usually classified as being transitions to one or the other of two limiting types of upper levels: Rydberg orbitals or virtual valence orbitals. The large, diffuse Rydberg orbitals collapse into the band structure of the solid upon chemisorption or solidification and are generally not observed. Thus Rydberg transitions in gas phase spectra can be identified readily by comparison to the spectrum of the same molecule in the solid state. The virtual valence orbitals can be classified as being of σ^* or π^* character, where for nonplanar molecules σ and π symmetry refer to the orientation of orbitals along or perpendicular to a particular C–C axis in the molecule. When the orientation of a molecule is fixed, as in chemisorption or in an oriented multilayer, a transition can be identified as either σ^* or π^* from the polarization dependence of the spectral intensity[5] if the molecular orientation on the surface is known or can be deduced. Of course "Ryd-

[a)] Present address: Surface Science Division, National Bureau of Standards, Gaithersburg, MD 20899.

 0021-9606/86/214849-14$02.10

berg" or "virtual valence" designations are limiting abstractions. In reality an upper state can have an intermediate, mixed Rydberg–valence character, as has been discussed extensively in valence excitation spectroscopy.[6] One means of estimating the degree of either Rydberg or virtual valence character in a particular state is to compare condensed and gas phase intensities. The more similar these are, the greater the localization of the upper state and thus the more valence-like it is. Thus the observation of intense, sharp features in the spectra of multilayer ices[7] and monolayer of NH_3[8] and H_2O[9] indicates that previous interpretations of solely Rydberg character for these core-excited states[10] is inappropriate and that a description which includes an appreciable valence character is more accurate. A rather complete discussion of the Rydberg/valence nature of the core-excited states of H_2O has been presented by Ramaker[11] who concludes that the antibonding valence character dominates both of the pre-edge features.

Recently studies have been reported on inner shell excitation in gas phase noncyclic aliphatic hydrocarbons[2,12] and in cyclic aromatics.[4] In order to provide further understanding of inner shell excitation in different environments we have carried out an investigation of some cycloalkanes and cycloalkenes. Gas phase, solid, and chemisorbed spectra were recorded for C_4H_8, C_5H_8, C_6H_{12} (or C_6D_{12}), and C_8H_8 while only gas phase spectra have been recorded for C_3H_6, C_5H_{10}, and C_6H_{10}. These spectra are interpreted with the aid of MS-$X\alpha$ calculations of the carbon *K*-shell excitation spectra of C_3H_6, C_4H_8, and C_6H_{12}.

The paper is organized as follows. Section II describes the experimental procedures used to obtain the ISEEL, and NEXAFS spectra while Sec. II A provides details of the multiple scattering calculations. In Secs. III A–III D the results for the saturated species are presented. Separate subsections discuss: the σ^* resonances (Sec. III B), the mixed Rydberg/valence $\pi^*(CH_2)$ feature (Sec. III C), and the polarization dependence of the condensed phase spectra of cyclobutane and cyclohexane (Sec. III D). The spectra of the unsaturated species are presented in Sec. IV, with subsections discussing: the interpretation of the gas phase spectra (Sec. IV A) and the polarization dependence of the condensed phase spectra of cyclopentene and cyclooctatetraene (Sec. IV B). In Sec. V the results are discussed in the context of the previously described relationship between σ^* resonance position and bond length. This is followed by some concluding remarks in Sec. VI.

II. EXPERIMENTAL

The experimental apparatus and techniques used to acquire the ISEELS spectra have been described in detail elsewhere.[11] The gases used were the vapors of commercially obtained, high purity liquid samples which were all used without further purification except for cyclooctatetraene, which was vacuum distilled before use to remove impurities. Air and volatile impurities in the liquids were removed by a series of freeze–pump–thaw cycles. The absolute energy scales were determined by calibrating the spectra to the $1s\rightarrow\pi^*$ transition in CO (C_3H_6, C_5H_8, C_6H_{10}, and C_8H_8), CO_2 (C_4H_8), C_2H_2 (C_6H_{12}) or C_2H_4 (C_5H_{10}). The energies of the $1s\rightarrow\pi^*$ transitions in these calibrant gases were taken to be 287.40(2) eV,[13] 290.7(1) eV,[14] 285.9(1) eV,[15] and 284.7(1) eV,[15] respectively.

The NEXAFS spectra were acquired using the grasshopper monochromator on beam line I-1 at the Stanford Synchrotron Radiation Laboratory. The procedure used to collect a spectrum has been described previously.[4,16] Both solid and monolayer spectra were measured on a Pt(111) crystal surface. The surface was cleaned by exposure to 10^{-7} Torr of oxygen at 870 K, followed by annealing at 1200 K in ultrahigh vaccum. Sulfur was removed by argon ion sputtering. Solids of C_4H_8, C_5H_8, C_6D_{12}, and C_8H_8 were prepared by exposing the Pt(111) crystal, kept at 100 K, to 1×10^{-7} Torr of the respective gases for 60 s (6 L). Monolayer spectra were obtained by heating the Pt(111) crystal with the condensed multilayers to temperatures of 170 K for C_5H_8 and C_6D_{12} and to 210 K for C_8H_8, just above the multilayer desorption temperature. All spectra were recorded with the crystal at 100 K.

A. Calculational procedures

The calculations of the absorption cross sections for the near edge region in cyclopropane, cyclobutane, and cyclohexane were carried out using the multiple scattering (MS) $X\alpha$ method.[17] The approach was the same as that used in recent calculations of the near edge region in ethylene[18] and benzene.[4] The molecular potential was obtained in a self-consistent MS-$X\alpha$ calculation with half an electron removed from the 1*s* orbital of one of the carbon atoms (transition state potential). The carbon sphere radii were chosen to overlap by 20% and a value of 0.8 a.u. was used for the hydrogen sphere radius. Partial waves up to $l=6$ were included for the outer sphere, up to $l=2$ for the carbon atoms and $l=0$ for the hydrogen atoms. For cyclobutane, the inclusion of the $l=1$ partial wave for hydrogen made negligible changes in the calculated cross sections. The bond lengths in cyclobutane were taken from the geometry reported by Almenningen and Bastiansen.[20] Calculations of cyclobutane were carried out for both the planar and puckered geometries. Cyclobutane is known to have a puckered geometry in its equilibrium configuration although the barrier separating the two puckered conformations is very small.[21] A puckering angle of 30° (the average of the IR[21] and NMR[22] values) was used in the calculations.

Absorption cross sections for transitions from the core level to the continuum states were calculated using the program of Davenport[23] with the acceleration form of the dipole operator. Oscillator strengths for bound state transitions were calculated by the method of Noodleman[24] and converted to cross sections using the relation[25]

$$\sigma(E)=\frac{\pi e^2h}{mc}\frac{df}{dE}=\frac{\pi e^2h}{mc}f\frac{dn}{dE},$$

where f is the oscillator strength and n is the principal quantum number. The height of the resonance is given by $\sigma(E)$ and the width by $(dn/dE)^{-1}$. The latter quantity was fixed at 1 eV, accounting for both natural linewidth and instrumental broadening. Thus the bound states are represented by Lorentzians of width 1 eV and height $\sigma(E)$. The contin-

uum cross sections for cyclopropane and cyclobutane were convoluted with a Lorentzian of 1 eV width. For cyclohexane the calculated continuum resonances were much narrower than the observed resonances. In this respect the cyclohexane results are similar to the results obtained previously for benzene.[4] Although the origin of the discrepancy between the calculated and observed resonance widths is not fully understood at present, it could be the result of additional vibrational broadening in these molecules. As for benzene,[4] the calculated cross section for cyclohexane was convoluted with a Lorentzian of 3 eV width to produce a simulated spectrum for comparison to experiment.

III. RESULTS AND DISCUSSION

A. Cyclic alkanes

The carbon *K*-shell spectra of gas phase C_3H_6 (cyclopropane), C_4H_8 (cyclobutane), C_5H_{10} (cyclopentane), and C_6H_{12} (cyclohexane) are shown in Fig. 1. The hatched lines indicate the onset of C 1*s* ionization. To our knowledge only the carbon *K*-shell ionization potentials (I.P.) of gaseous cyclopropane and cyclohexane have been reported.[26] The C 1*s* I.P.'s of saturated hydrocarbons systematically decrease with increasing size so the I.P.'s of cyclobutane and cyclopentane are expected to lie between these two values and are estimated to be 290.5 and 290.4 eV, respectively. These estimates should be accurate within 0.2 eV. Except for the weak peak (a) at 284.6 eV in cyclobutane, which is attributed to the intense $1s\rightarrow\pi^*$ feature in C_2H_4[15] formed in the decomposition of cyclobutane, all spectral features are interpreted as transitions to unoccupied levels of the cyloalkanes. The energies, term values, and proposed assignments are listed in Table I.

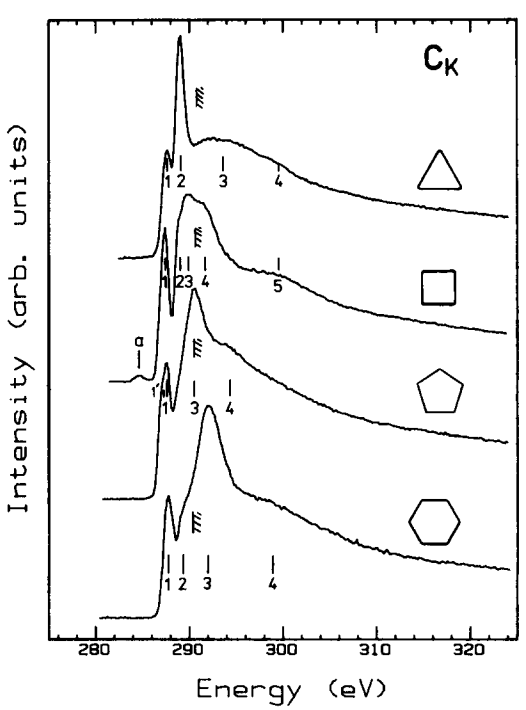

FIG. 1. The carbon *K*-shell ISEEL spectra of gaseous cyclopropane, cyclobutane, cyclopentane, and cyclohexane recorded by electron energy loss of 2.8 keV electrons at 0.7 eV FWHM resolution.

B. σ^* Resonances

The most intense features in the spectra of the cycloalkanes occur around the C 1*s* I.P. These features are assigned to $1s\rightarrow\sigma^*$(C–C) transitions. The occurrence of the majority of the σ^* resonance intensity around the I.P. is consistent with the C–C bond lengths of the cycloalkanes[27] within the previously described correlation of bond lengths and resonance positions.[2] The details of the correlation are discussed in Sec. V. The MS-$X\alpha$ calculations for cyclopropane, puckered cyclobutane, and cyclohexane (chair confirmation) are shown in Fig. 2 in comparison with the experimental gas phase ISEELS spectra. For each of these molecules the calculated spectrum shows several σ^* resonances with the first resonance being close to the I.P. and considerably more intense than the δ^* resonance(s) at higher energy. The calculated spectrum for planar cyclobutane is almost identical to the spectrum for the puckered molecule although the resonances are somewhat sharper in the planar geometry.

Apart from some weak features which are not reproduced by the MS-$X\alpha$ calculation, the experimental and calculated spectra of cyclopropane and cyclobutane in the region of σ^* resonances are in reasonable agreement whereas there is somewhat worse agreement between theory and experiment for cyclohexane. The two σ^* features calculated for cyclobutane have positions and relative intensities in good agreement with the observed features. The calculated continuum of cyclopropane contains one feature whereas there is a distinct shoulder around 300 eV on the high energy side of the broad continuum resonance in cyclopropane. The calculated continuum of cyclohexane exhibits three σ resonances in contrast to the experimental observation of only two resonances.

The calculated polarization dependence of the σ^* resonances in cyclopropane and cyclobutane gives insight into the character of these upper states. Following the same procedure used to assign the resonances in benzene,[4] we define local x and y axes on each carbon atom, with the x axis pointing towards the center of the ring and the y axis perpendicular to it in the plane of the molecule. For both molecules the most intense resonance (#2 in cyclopropane, #3 in cyclobutane) is obtained only for radiation with the E vector parallel to the y axis on the excited carbon atom. This means that the upper level is a_2' in cyclopropane and a_{2g} in planar cyclobutane. In both cases these molecular orbitals are obtained from an antibonding combination of p orbitals oriented along the local y axes (see scheme 1). The spatial distribution of these orbitals is well represented in the work of Jorgensen and Salem.[28]

scheme 1

TABLE I. Absolute energies and proposed assignments of features observed in the carbon *K*-shell spectra of cyclopropane, cyclobutane, cyclopentane, and cyclohexane.

	Cyclopropane				Cyclobutane[a]		
#	*E* ± 0.1 eV	*T*[b] eV	Assignment final orbital	#	*E* ± 0.1 eV	*T*[b] eV	Assignment final orbital
				a	284.6(2)		π^* in C_2H_4
1	287.7	2.9	$4a_1' \pi^*$ (CH_2)	1	287.4[d]	3.1	$2a_{2u}\pi^*$ (CH_2)
2	289.0[c]	1.6	$a_2'\sigma^*$ (C–C)	2	288.9	1.6	$4p$
				3	289.9	0.6	$1a_{2g}\sigma$ (C–C)
I.P.	290.6[e]			I.P.	290.5[f]		
3	293.2(8)	−2.6	$e'\sigma^*$ (C–C)	4	291.6(5)	−1.1	$4e_u\sigma^*$ (C–C)
4	299.2(8)	−8.6	σ^* (C–C)	5	299.2(8)	−8.7	$4b_{2g}\sigma^*$ (C–C)
	Cyclopentane				Cyclohexane[g]		
1′	287.0	3.4	$3s$				
1	287.6[h]	2.8	$14a'\pi^*$ (CH_2)	1	287.7[i]	2.6	$4a_{1u}\pi^*$ (CH_2)
					2	289.2	1.1
$4p$							
I.P.	290.4[f]				I.P.	290.3[e]	
3	290.5	−0.1	$9a''\sigma^*$ (C–C)	3	291.9	−1.6	$a_{2u}\sigma^*$ (C–C)
4	294.5(8)	−4.1	$13a'\sigma^*$ (C–C)	4	299.6(8)	−9.3	σ^* (C–C)

[a] Orbital designation based on the average planar structure (D_{4h}). The lowest energy configuration is puckered (D_{2d}) but the barrier to inversion is small.
[b] T = I.P. − E. (Note in Table VI, $\delta = -T$.)
[c] This feature is located 1.60(5) eV below the π^* transition in CO (Ref. 13).
[d] This feature is located 3.30(6) eV below the π^* transition in CO_2 (Ref. 14).
[e] From x-ray PES (Ref. 26).
[f] Estimated by interpolating between the I.P.'s of cyclopropane and cyclohexane (Ref. 26).
[g] Orbital designations are based on the chair conformation (D_{3d}).
[h] This feature is located 2.85(9) eV above the π^* transition in C_2H_4 (Ref. 15).
[i] This feature is located 1.81(9) eV above the π^* transition in C_2H_2 (Ref. 15).

The higher resonance in the case of cyclopropane (#3) is obtained when the E vector is parallel to either the x or y axis (although the x axis component is by far the stronger). The upper level can therefore be assigned to be e'. For cyclobutane the higher energy calculated resonance is intense only for radiation with the E vector parallel to the x axis. Thus the upper level for this transition must be the b_{2g} orbital which is formed from an antibonding combination of the p orbitals pointing towards the center of the ring (scheme 2).

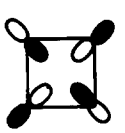

scheme 2

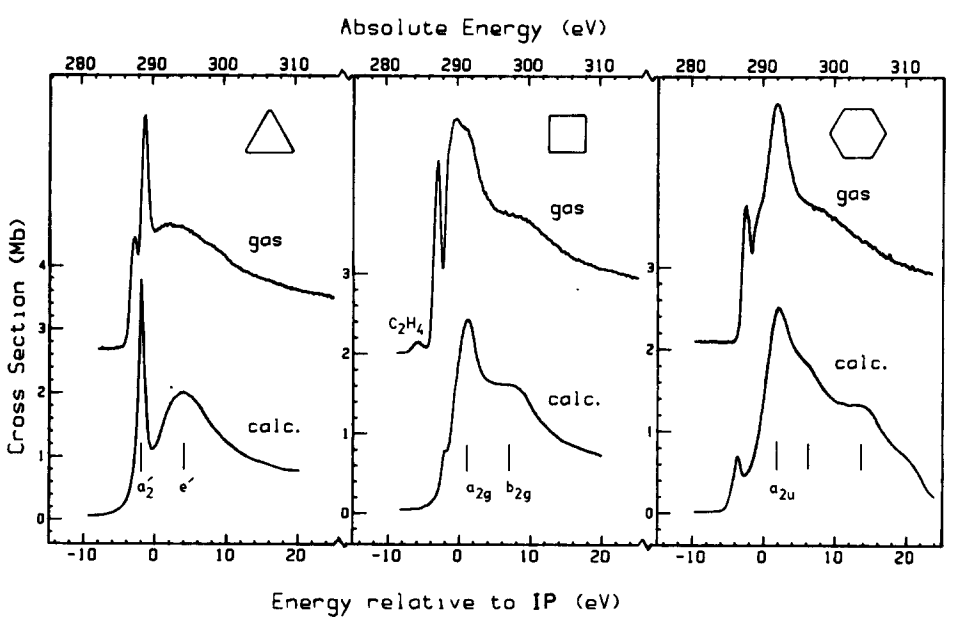

FIG. 2. Comparison of the gas phase ISEELS and MS-$X\alpha$ calculated carbon *K*-shell spectra of cyclopropane, cyclobutane, and cyclohexane. The cross sections are computed per carbon atom and do not include any contribution from underlying valence ionization.

Note that for cyclopropane the description of e' in terms of "Walsh orbitals" also consists of *sp* hybrids pointing towards the center of the ring. The upper states of the two principal resonances in cyclopropane (#2, #3) are therefore analagous to the upper states for the corresponding resonances in cyclobutane (#3, #5). For cyclobutane one more low-lying state is expected from a simple MO treatment, that of e_u symmetry. There is no calculated feature that can be assigned to this state. We suggest that it may correspond to the weak feature (#4) at 291.6 eV, on the high energy side of the intense a_{2g} resonance at 289.9 eV (#3). A similar description of the occupied and unoccupied valence orbitals of cyclopropane and cyclobutane had been presented by Hoffman and Davidson[29] who explain the unusual reactivity of these species in terms of their orbital character.

The ordering of σ^* levels predicted by the MS-$X\alpha$ calculations ($a_2' < e'$) differs from that given by the *ab initio* calculation of Basch *et al.*[30] for which the orbital energies and electron densities are summarized by Jorgensen and Salem.[28] However the ordering and the energy separation (6.2 eV) obtained in this work are both in good agreement with the *ab initio* results of Buenker and Peyerimhoff.[31] The disagreement of different *ab initio* calculations with regard to the order of virtual levels probably reflects the sensitivity of Hartree–Fock methods to the choice of basis set. According to the MS-$X\alpha$ results the σ^* resonances occur predominantly with $l = 3$ outer sphere components in cyclopropane and $l = 4$ in cyclobutane.

We note that the a_2' orbital in cyclopropane is the upper level of an exceptionally intense resonance, known as a "giant resonance", in the VUV spectral region.[32] In this case the transition starts from an e' valence orbital rather than a C 1*s* orbital and the observed VUV spectrum[46] exhibits two strong resonances at 10.2 and 13.0 eV which are interpreted as the Jahn–Teller split components of the $(3e'^{-1}, 1a_2')\ ^1E'$ state. There is a similar giant resonance of a_{2u} symmetry in the VUV spectrum of cyclohexane, lying just above the ionization threshold. The corresponding feature in the x-ray region is the intense resonance (feature 2) located 1.6 eV above the I.P. Based on the VUV assignment we assign feature 2 in the C 1*s* spectrum of cyclohexane to C $1s \rightarrow a_{2u}$ transitions. This aspect of the spectrum of cyclohexane has been discussed previously.[33]

The experimental and calculated results of these molecules suggest that the C 1*s* spectra of cycloalkanes do not follow fully the simple relationship of one continuum resonance per bond length between heavy atoms proposed from earlier studies.[2,12] Although the most intense resonance generally occurs at an energy consistent with the correlation, additional σ^* features do occur. These additional continuum features can be considered to arise from interactions among several localized σ^*(C–C) states at similar energies. Such interactions produce several delocalized states separated in energy thus producing a wider distribution of σ^*(C–C) oscillator strength. In both calculation and experiment the intensity of the higher energy σ^* resonance(s) in the cycloalkanes decreases in the order: cyclopropane, cyclobutane, cyclohexane, suggesting a systematic decrease in its intensity as ring size increases. The decrease in intensity of the additional feature with increasing ring size is consistent with an origin associated with interactions among σ^* levels since the greater distance between bonds and the less rigid geometry of the larger molecules lessens the interaction. A similar trend of decreasing intensity of a second, higher energy σ^*(C–C) transition with increasing ring size has been observed in recent studies of both saturated heterocyclics[34] and linear alkanes.[35] Several resonances arising from delocalized σ^* states are also observed in the C 1*s* continua of benzene, pyridine,[4] and borazine[33] whereas the simple bond length correlation predicts only a single σ^*(C–C) feature in each of these molecules.

A possible alternate assignment for the higher energy continuum features is to σ^* levels associated with C–H bonds. Continuum features have been assigned in this manner in the *K*-shell continua of CH_4, NH_3, and H_2O.[2] However this feature gets noticeably weaker as the size of the hydrocarbon ring increases whereas a σ^*(C–H) transition would be of constant intensity or possibly become stronger because of the greater number of C–H bonds. Both the incorrect ring size dependence and the variable position contradict a σ^*(C–H) interpretation based on the bond length correlation concepts. Of course the separation of continuum resonances into localized σ^*(C–C) and σ^*(C–H) is only a first approximation and the resonances will have mixed character in most cases. Other possible assignments for the second continuum features include double excitation (simultaneous excitation of both a valence and core electron) or shakeup (ionization plus excitation). Double excitation transitions are generally much sharper than this feature. The width is more consistent with a very short lived state arising from a one-electron promotion (as assigned) or possibly, a shakeup continuum. The onset of shakeup continua in ISEELS should correspond to the position of peaks in XPS satellite spectra. The XPS satellite spectra of these molecules have not been reported to our knowledge. However, in previous comparisons for many other molecules there has been little correlation between onsets of continuum features and XPS satellites. This is not surprising since the shakeup process is likely very weak at threshold. Thus we feel that essentially all of the continuum features arise from one-electron excitations to σ^*(C–C) levels as assigned in Table I.

C. The mixed Rydberg/valence π^* (CH_2) state

This section deals with the interpretation of peak 1 in the spectra of the cycloalkanes (Fig. 1). Overall this feature is well aligned in all four spectra and has a term value between 2.6 and 3.1 eV. This is in the range expected for transitions to 3*p* Rydberg states.[36] However peak 1 is assigned to a mixed Rydberg/valence state rather than a pure Rydberg state, based on the relative intensity and polarization dependence of the corresponding feature observed in the condensed phase spectra of cyclobutane and cyclohexane. The NEXAFS spectra of solid cyclobutane [in the form of a multilayer ice on a Pt(111) surface] recorded with both normal (90°) and glancing (20°) incidence are shown in Fig. 3 in comparison to the gas phase ISEEL spectrum. Monolayer spectra of cyclobutane could not be obtained because all of

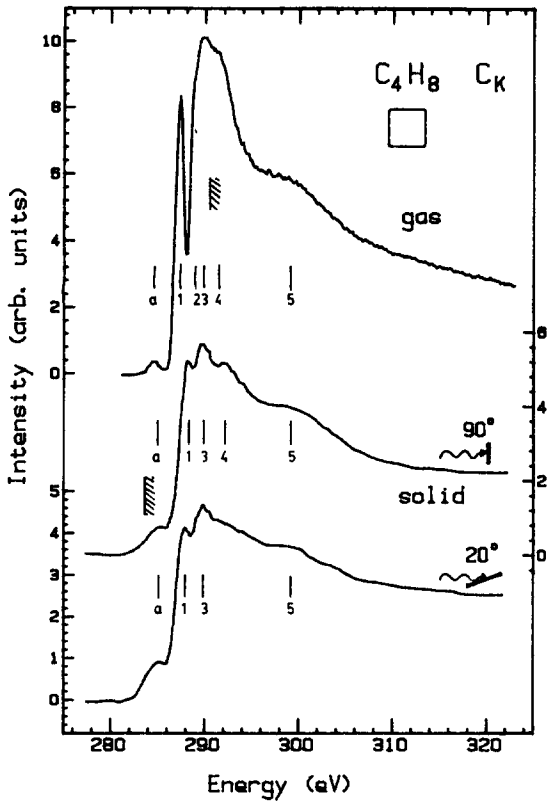

FIG. 3. (a) The carbon *K*-shell ISEEL spectrum of gaseous cyclobutane. (b) The carbon *K*-shell NEXAFS spectrum of solid cyclobutane recorded with normal x-ray incidence by partial electron yield from a multilayer condensed on Pt(111) at 100 K. (c) The glancing incidence NEXAFS spectrum of solid cyclobutane. A background estimated from the shape of the low energy pre-edge region has been subtracted from the original data to produce the spectra shown.

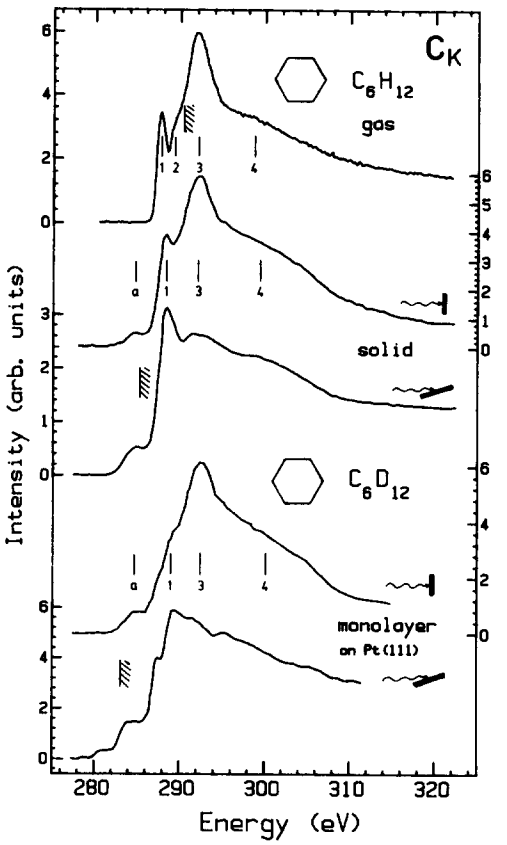

FIG. 4. (a) The carbon *K*-shell ISEEL spectrum of gaseous cyclohexane. (b) The carbon *K*-shell NEXAFS spectrum of solid cyclohexane (*d*-12) recorded with normal x-ray incidence by partial electron yield from a multilayer condensed on Pt(111) at 100 K. (c) The glancing incidence NEXAFS spectrum of solid cyclohexane (*d*-12). (d) The normal incidence NEXAFS specrum of a monolayer of deuterated cyclohexane on Pt(111) produced by heating the multilayer sample to 170 K. (e) The glancing incidence NEXAFS spectrum of a monolayer of deuterated cyclohexane on Pt(111) (heated to 170 K). The hatched lines indicate the C 1*s* ionization energies of the gas (relative to the vacuum level), the solid (relative to the Fermi level of polycrystalline gold), and the monolayer on Pt(111) [relative to the Fermi level of the Pt(111) surface]. The spectra shown have had a background subtracted.

the multilayer desorbed upon warming. The NEXAFS spectra of solid (multilayer) and monolayer cyclohexane on Pt(111), each recorded at both normal (90°) and grazing (20°) x-ray incidence, are shown in Fig. 4 along with the gas phase spectrum for comparison. The hatched lines in Figs. 3 and 4 indicate the locations of the ionization thresholds as measured by XPS.[26,37] The NEXAFS spectra of cyclohexane were recorded using C_6D_{12} rather than C_6H_{12}. Although a deuterium isotope effect has been observed in the carbon *K*-shell spectrum of methane,[38] the spectrum of C_6D_{12} is not expected to differ significantly from that of C_6H_{12}. Energies and proposed assignments of the features in the condensed phase spectra of both cyclobutane and cyclohexane are listed in Table II.

The prominent intensity of the feature labeled #1 in both the multi- and monolayer spectra (Figs. 3 and 4) is inconsistent with a solely 3*p* Rydberg assignment since transitions to Rydberg orbitals generally disappear in condensed phase spectra. Indeed, this behavior is used frequently to distinguish valence from Rydberg transitions.[36] Furthermore, peak 1 shows polarization dependence in the spectra of both multi- and monolayer cyclohexane which would not be expected for a transition to a spherically symmetric Rydberg orbital (at our experimental resolution components of a symmetry-split 3*p* Rydberg state would be unresolved). Although the first transition in solid cyclobutane is less well resolved than in the gas phase and does not exhibit polarization dependence, it is clearly detected. These aspects of the condensed phase spectra of cyclobutane and cyclohexane rule out a purely 3*p* Rydberg assignment for feature 1.

The obvious alternative is to assign feature 1 in both molecules to transitions to a state of mixed Rydberg/valence character in which the valence character dominates for excitations from the localized carbon 1*s* level. This would be consistent with both the polarization and the strong intensity in the condensed phase spectra. Cyclohexane in the chair conformation has a low lying antibonding $4a_{1u}\pi^*$ (CH_2) orbital[28] and transitions to this level are dipole allowed. Furthermore, peak 1 shows a polarization dependence which is opposite of that of the σ^*(C–C) shape resonance (#3), as would be expected for an upper state involving population of an orbital oriented perpendicular to the C–C bond. Thus both the polarization dependence and the absence of quenching in the solid state are consistent with a predominantly $4a_{1u}\pi^*$ (CH_2) character to the upper level. Cyclo-

TABLE II. Absolute energies and proposed assignments of features observed in the carbon *K*-shell spectra of gas and multilayer C_4H_8 on Pt(111) and gas, multilayer, and monolayer C_6H_{12} on Pt(111).

Cyclobutane

Feature final orbital	Gas ±0.1 eV	Multilayer 90° ±0.5 eV	Multilayer 20° ±0.5 eV	Assignment
a	284.6	285.0(8)	285.5(8)	see the text
1	287.4	288.2	288.0	$2a_{2u}\pi^*$ (CH_2)
2	288.9			$4p$
3	289.9	290.0	290.0	$a_{2g}\sigma^*$ (C–C)
I.P.	290.5[a]	283.8[b]	283.8[b]	
4	291.6	292.0		$4e_u\sigma^*$ (C–C)
5	299.2(8)	300 (1)	300 (1)	$4b_{2g}\sigma^*$ (in-ring)

Cyclohexane

Feature	Gas ±0.1 eV	Multilayer 90° ±0.5 eV	Multilayer 20° ±0.5 eV	Monolayer 90° ±0.5 eV	Monolayer 20° ±0.5 eV	Assignment final orbital[c]
a	···	284.5(8)	284.5(8)	285(1)	284(1)	see the text
1	287.7	288.2	288.5	289.4	289.4	$4a_{1u}\pi^*$ (CH_2)
I.P.	290.3[d]	285.4[e]	285.4[e]	283.5[f]	283.5[f]	
3	291.9	292.2	291.5	292.6	···	$a_{2u}\sigma^*$ (C–C)
4	299.6	301.6	300.5	···	···	σ^* (in-ring)

[a] Estimated from the I.P.'s of cyclopropane and cyclohexane (Ref. 26).
[b] From XPS (Ref. 37)—binding energy relative to the Fermi level of Pt(111).
[c] Orbital designation for the chair conformation (D_{3d}).
[d] From XPS (Ref. 26).
[e] From XPS (Ref. 45)—binding energy relative to the Fermi level of polycrystalline Au.
[f] From XPS (Ref. 37)—binding energy relative to the Fermi level of Pt(111).

pentane also has a low-lying unoccupied $14a'\pi^*(CH_2)$ orbital[28] suggesting this assignment for peak 1 in that spectrum. In cyclobutane the lowest unoccupied MO is the $2a_{2u}$ $\pi^*(CH_2)$ in a planar geometry while in cyclopropane the corresponding MO is of $4a_1'$ symmetry.

In contrast to the reasonable agreement between calculation and experiment for the σ^* resonances, there is relatively poor agreement for the bound states below the C 1*s* I. P. (Fig. 2). Weak features are observed 2.1 and 3.8 eV below the I.P. in the calculated spectra of cyclobutane and cyclohexane which roughly match the $3p/\pi^*$ (CH_2) features (experimental term values of 3.1 and 2.6 eV). In cyclopropane the lowest energy peak is not reproduced as a distinct feature by the MS-$X\alpha$ calculation although a weak transition is calculated to overlap the intense a_2' resonance. For all species the calculated cross section of this transition is much smaller (relative to the continuum) than observed experimentally. It appears that the calculational procedures are not adequate to reproduce the discrete structure in these molecules, where extensive Rydberg–valence mixing seems to occur. This situation is qualitatively different from unsaturated species such as ethylene,[18] benzene,[4] etc. where the MS-$X\alpha$ method gave good agreement with experiment for both the discrete and continuum regions.

The MS-$X\alpha$ calculations indicate that feature 1 in cyclobutane and cyclohexane corresponds to excitations to the second lowest unoccupied orbital. The lowest energy excitation is calculated to be a very weak C 1*s*→3*s* transition. The upper state for feature 1 is calculated to have a mixed Rydberg–valence character with the Rydberg character predominating at the ground state geometry. Such mixed Rydberg–valence states are well-known for small hydride molecules. They occur when a Rydberg orbital has the same nodal pattern as one of the antibonding valence orbitals. For example, the 3*s* Rydberg orbital in H_2O and NH_3 mixes with the O–H and N–H σ^* orbitals, with the amount of mixing being very dependent on the O–H and N–H distances.[9,39] As the O–H or N–H distance increases, the antibonding component increases and the mixed state changes from predominantly Rydberg to predominantly valence antibonding. The mixed Rydberg–valence character of the upper state of feature 1 in cyclopropane and cyclobutane can be shown by the change in the composition of the upper state when the C–H distance is increased. For cyclopropane, at the ground state geometry the percentage of the electronic charge contained in the atomic spheres and the inter and outer sphere regions is: C 8%, H 0%, inter 12% and outer 79%. With an increase of only 10 pm in the C–H distance the percentages become: C 12%, H 0.5%, inter 16% and outer 71%. The Rydberg character of the orbital is evident from the large outer sphere contribution, which is typically 10%–20% for purely valence orbitals. The removal of charge from the outer sphere

and its transfer to the carbon atoms as the bond length increases corresponds to a decrease in the Rydberg character of the orbital (measured by the amount of charge in the outer sphere region) and an increase in the valence character. However the MS-$X\alpha$ calculations for these mixed Rydberg–valence states predict a much lower intensity than that observed.

For cyclobutane the calculations give only a weak shoulder on the side of the first continuum resonance instead of the very strong peak in the experimental spectrum. The calculated $3p/\pi^*$ (CH_2) feature in cyclopropane falls at almost exactly the same energy as the intense a_2' resonance and so does not appear as a separate feature. Evidently the contribution of the Rydberg component of the mixed state is overestimated by the calculations. The reasons for the failure of the calculations to describe the mixing in this state are not clear. It could be that the relative contributions of the Rydberg and valence states are very sensitive to the accuracy of the calculation and that a one-electron self-consistent-field treatment is not accurate enough to give a good description of these states. One electron calculations do appear to be adequate for the description of similar mixed states observed in the VUV spectra of small hydride molecules such as H_2O and NH_3,[39] but the core hole may cause changes in the Rydberg/valence mixing that can be described only by more accurate calculations. Alternatively the discrepancy could be due to vibronic effects. The C–H distance in the upper state could be significantly longer than in the ground state. This seems reasonable in view of the antibonding π^* (CH_2) character of the upper state. Vertical Franck–Condon transitions from points on the ground state potential surfaces corresponding to C–H bond lengths somewhat greater than the equilibrium value would now have significant intensity. The antibonding valence component in the upper state increases with increasing C–H distance, so such transitions could dominate the observed spectrum. A calculation using the ground state geometry would not therefore reproduce the observed intensity.

A reassignment of the previously reported C 1*s* spectra of other saturated hydrocarbons is suggested by the present assignment of the first feature in the spectra of C_3H_6, C_4H_8, C_5H_{10}, and C_6H_{12} to transitions to a level of predominantly π^* (CH_2) character. For example, molecular orbital diagrams for ethane show that an analogous π^* (CH_3) orbital exists in both the staggered and eclipsed conformations of ethane.[28] Thus we suggest that the intense feature at 287.9 eV in the carbon *K*-shell spectrum of ethane[15] corresponds to transitions to an upper level of predominantly π^* (CH_3) rather than 3*p* Rydberg character. The C 1*s* NEXAFS spectrum of ethane condensed on Cu(100) exhibits a corresponding feature,[40] providing additional support for this reassignment. A similar feature, also assigned to transitions to a level of predominantly π^* (CH_2) character, is observed in the C 1*s* spectra of a number of linear and branched alkanes,[35] further supporting the present assignment.

The shoulder (#2) on the low energy side of the main σ^*(C–C) feature in both the C_4H_8 and C_6H_{12} spectra is assigned on the basis of its term value ($\sim$1.5 eV) to an incompletely resolved 4*p* Rydberg transition. Interestingly the C $1s\rightarrow 3s$ transition, which is expected to have a term value of about 3.5 eV, is only observed in cyclopentane (#1′ in Fig. 1) and not in the other cycloalkanes. This is considerably different than the spectra of the corresponding linear alkanes[35] where the 3*s* feature is observed in all cases, with an intensity relative to the π^* (CH_2) transition which increases as the chain length increases. The C $1s\rightarrow 3s$ transition in cyclopropane, cyclobutane, and cyclohexane could be hidden underneath a broadened and lower energy π^* (CH_2) transition. However the measured widths (FWHM) of the π^* (CH_2) features are essentially identical in the corresponding C_nH_{2n} cyclic and C_nH_{2n+2} noncyclic alkanes, with the width increasing systematically from 1.1 eV in cyclopropane/propane to 1.5 eV in cyclohexane/hexane. The apparently very weak intensity of the C $1s\rightarrow 3s$ transitions in cycloalkanes is also predicted by the MS-$X\alpha$ calculations.

D. Further discussion of the solid and monolayer spectra of C_4H_8 and C_6H_{12}

The NEXAFS spectra of multilayer cyclobutane (Fig. 3) and those of multi- and monolayer cyclohexane (Fig. 4) exhibit further features noteworthy both with regard to spectroscopic assignments and to the electronic and geometric structure of these condensed phases. Aside from resolution differences the condensed and gas phase spectra of cyclobutane are very similar, as are those of cyclohexane. This indicates that most of the features arise from transitions to a common set of localized unoccupied molecular levels. There is very little polarization dependence of the spectrum of solid cyclobutane which indicates that the molecules are oriented randomly in the multilayer. One obvious difference between the spectra of gas and solid cyclobutane is the relative intensities of the feature around 285 eV marked (a) in Fig. 3. The feature at this energy in the gas phase spectrum of cyclobutane is relatively narrow and is believed to be the C $1s\rightarrow\pi^*$ transition in C_2H_4 arising from decomposition of cyclobutane. The 285 eV feature in the solid state is considerably more intense and appears to be more of a continuum onset rather than an actual peak. Relative to the σ^*(C–C) resonances the intensity of (a) varies with x-ray incidence. The variation is consistent with that expected from a $1s\rightarrow\pi^*$ transition in an ethylene molecule oriented parallel to the surface. However, relative to the nonstructured continuum at 315 eV there is negligible intensity variation of (a) with polarization changes. Thus the polarization dependence of this feature is ambiguous.

In the gas phase spectrum of cyclohexane only a smooth valence ionization continuum is observed at 285 eV in the region of feature (a) whereas the multi- and monolayer spectra (Fig. 4) both exhibit exhibit a feature similar to the bump seen in solid cyclobutane. The fact that (a) is observed only in the condensed phase spectra suggests that it arises from intermolecular or molecule–surface interactions. In monolayer cyclohexane, (a) could arise from promotion of carbon 1*s* electrons into the unoccupied valence band of the metal substrate. This interpretation is supported by the observation that the threshold of (a) is almost coincident with the measured C *K*-shell I.P.,[37] corresponding to the Fermi level of C_6D_{12} covered Pt(111). The cyclohexane multilayer

is probably very thin since the 6 L exposure would correspond to ~6 layers if the sticking coefficient was unity and the sticking coefficient will be smaller on cyclohexane than on clean Pt(111). Relative to the higher energy features, (a) is weaker in the multilayer than in the monolayer. This suggests that (a) may arise from transitions to metal valence band or molecule–surface states in the C_6D_{12} layer closest to the metal. This signal, detected in a partial electron yield mode, would in a sense be "shining through" the overlying C_6D_{12} layers. A patchy multilayer could also explain the observation of signal from monolayer regions. Alternatively this feature could arise from ethylene impurity (or another unsaturated species such as benzene which also has a π^* state around 285 eV). However the observation of similar features in both cyclobutane and cyclohexane (the only cyclic alkanes whose NEXAFS has been studied to date) and the absence of any other evidence of impurities either in the gas samples or on the Pt(111) surface prior to adsorption suggests that these features are characteristic of cyclobutane or cyclohexane adsorbed on a Pt(111) surface.

Surprisingly, the spectrum of *multilayer* C_6D_{12} shows considerable variation with angle of x-ray incidence. This suggests that it is at least partially oriented, indicating epitaxial crystal growth of the multilayer. The degree of orientation in a sample can be expressed by an orientation factor defined as the ratio of the intensity of a feature in spectra recorded with different angles of x-ray incidence on the sample. Since absolute intensities have not been measured, the intensity ratios were normalized by taking the ratio of peak 3 to peak 1 in the normal incidence and glancing incidence spectra of multilayer C_6D_{12}. This ratio should be 1 if the multilayer was randomly oriented. The measured orientation factor of 0.16 indicates considerable orientation. Initially the polarization variation of the multilayer spectrum was considered to be the effect of a thin multilayer allowing the highly oriented monolayer signal to shine through a less oriented overlayer. This is consistent with the greater polarization dependence of the monolayer spectra than of the multilayer spectra of C_6D_{12}. The orientation factor as defined above is 0.08 for the monolayer. However this interpretation is inconsistent with the observation that peak 1 in the multilayer spectrum is much sharper than its counterpart in the monolayer spectrum. It appears that flexible, weakly interacting molecules such as cyclohexane can reorient while condensing much more easily than rigid, strongly adsorbed molecules such as benzene, pyridine,[4] thiophene,[41] cyclobutane, or the unsaturated cyclic hydrocarbons, C_5H_8 and C_8H_8 (see Figs. 6 and 7). From their spectra it appears that all of these latter species form disordered multilayers with little or no polarization dependence whereas cyclohexane reorients during or after condensation and undergoes epitaxial growth. The increased mobility of cyclohexane under the conditions used for multilayer formation can be attributed to the fact that the temperature of the Pt(111) substrate during condensation is much closer to T_{vap} of cyclohexane than to T_{vap} of the other species studied.

The enhancement of peak 3 in the normal incidence spectra of cyclohexane (Fig. 4) is characteristic of a σ^* resonance in a molecule whose bond axis lies approximately parallel to the Pt(111) surface. The reduction of peak 1 in the normal incidence spectra and enhancement of this feature in the glancing incidence spectra is characteristic of a π^* resonance in a molecule lying parallel to the surface. As discussed in the previous section, this observation supports our assignment of this feature to a state of predominantly π^* (CH_2) character. The π^* (CH_2) feature (#1) is considerably broader in the monolayer spectrum than in the gas phase or multilayer spectra. This indicates broadening of the π^* (CH_2) level by hybridization into metal levels as previously observed and discussed for the π^* (C=C) level in benzene.[4]

IV. CYCLIC ALKENES

A. Gas phase spectra

The gas phase ISEELS spectra of cyclopentene, cyclohexene, and cyclooctatetraene are shown in Fig. 5. The spectra of cyclopentene and cyclohexene were recorded at somewhat lower resolution (1.0 eV as opposed to 0.6 eV FWHM). Absolute energies and assignments for cyclopentene and cyclohexene are listed in Table III while those for cyclooctatetraene are listed in Table V. The carbon *K*-shell I.P. of each of these molecules is estimated to be 290.4 eV in the gas phase from comparison to other hydrocarbons.

In all three spectra an intense peak corresponding to $1s \rightarrow \pi^*$ (C=C) transitions is observed around 285 eV. The

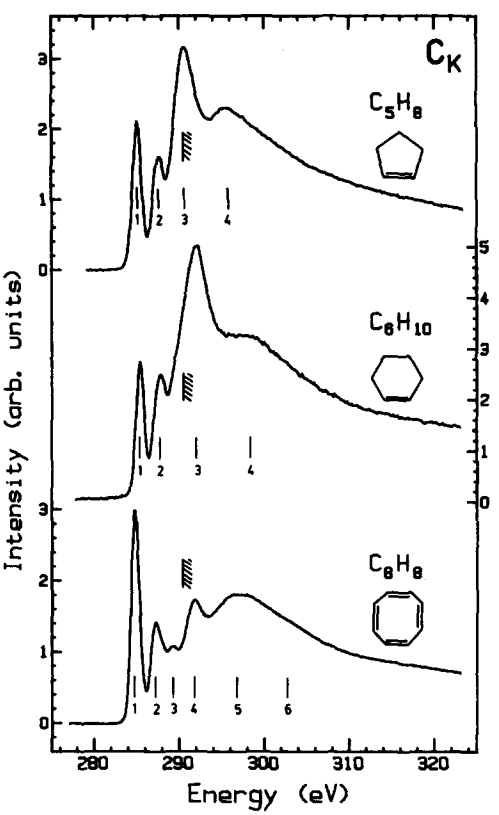

FIG. 5. The carbon *K*-shell ISEEL spectra of gaseous cyclopentene, cyclohexene, and cyclooctatetraene recorded by electron energy loss of 2.8 keV electrons. The spectra of cyclopentene and cyclohexene were recorded with 1.0 eV FWHM resolution while that of cyclooctatetraene was obtained with 0.6 eV FWHM resolution.

TABLE III. Absolute energies and proposed assignments of features observed in the carbon *K*-shell spectra of gaseous cyclopentene and cyclohexene.

Feature	C_5H_8 Energy	C_5H_8 T	C_6H_{10} Energy	C_6H_{10} T	Assignment final orbital
1	285.0[a]	5.4	285.3[b]	5.1	π^* (C=C)
2	287.6	2.8	287.7	2.7	π^* (CH_2)
I.P.	290.4[c]		290.4[c]		
3	290.6	−0.2	292.0	−1.6	σ^* (C–C)
4	295.6	−5.2	298.5	−8.1	σ^* (C=C)

[a] This feature is located 2.38(4) eV below the π^* transition in CO (Ref. 13).
[b] This feature is located 2.12(9) eV below the π^* transition in CO (Ref. 13).
[c] Estimated from the I.P.'s of similar hydrocarbons (Ref. 26).

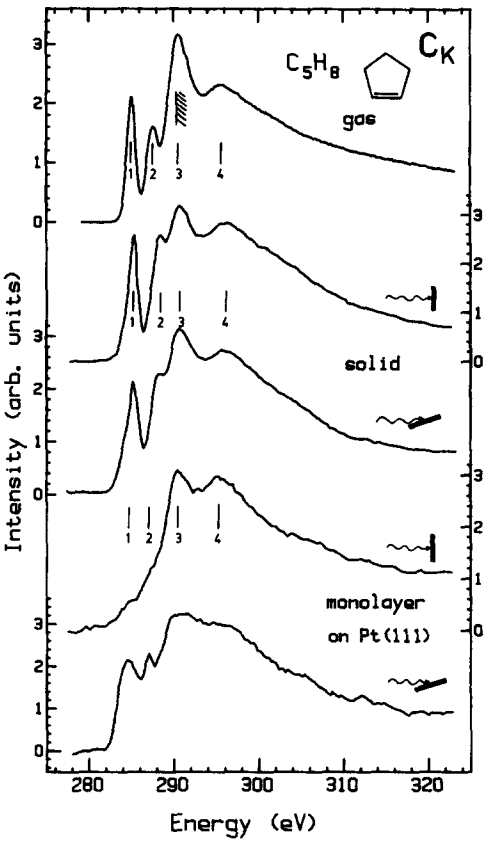

FIG. 6. The carbon *K*-shell ISEEL spectrum of gaseous cyclopentene. (b) The carbon *K*-shell normal incidence NEXAFS spectrum of solid (multilayer) cyclopentene condensed at 100 K. (c) The glancing incidence NEXAFS spectrum of solid (multilayer) cyclopentene condensed at 100 K. (d) The normal incidence NEXAFS spectrum of a monolayer of cyclopentene on Pt(111) produced by heating the sample to 170 K. (e) The glancing incidence NEXAFS spectrum of a monolayer of cyclopentene on Pt(111) (heated to 170 K). The spectra shown have had a background subtracted.

intensity of this peak relative to the continuum varies considerably. It is most intense in C_8H_8 and weakest in C_6H_{10} as expected since C_8H_8 contains a greater number of carbon–carbon double bonds. The term values of feature 2 in the gas phase spectra of C_5H_8 and C_6H_{10} are similar to that of feature 1 in the gas phase spectra of the cycloalkanes. Thus these features are assigned to a state of predominantly π^* (CH_2) character associated with the saturated regions in these molecules. Feature 3 in cyclopentene and cyclohexene and feature 4 in C_8H_8 are assigned to transitions to the σ^*(C–C) state. The positions of these features correlate with the C–C single bond length within the empirical relationship described previously.[2] The intensity of the σ^*(C–C) shape resonance relative to the π^* feature (#1) is highest in C_6H_{10}, consistent with this molecule containing the greatest number of carbon–carbon single bonds. Feature 4 in C_5H_8 and C_6H_{10} and feature 5 in C_8H_8 are assigned to a σ^* state associated with the shorter carbon–carbon double bonds. The variation in the intensity of this feature through this series of molecules is consistent with the σ^*(C=C) assignment since this feature is most intense in C_8H_8, the molecule with the greatest number of double bonds. Additional σ^*(C–C) states corresponding to the weak continuum features observed at higher energy in the cycloalkane spectra probably also contribute in the region of the σ^*(C=C) resonances of cyclopentene and cyclohexene.

In addition to variations in the relative intensities of the σ^*(C–C) and σ^*(C=C) continuum features, the discrete region of the gas phase spectrum of C_8H_8 differs considerably from that of C_5H_8 or C_6H_{10}. Cyclooctatetraene is a nonaromatic, unsaturated cyclic system whose most stable conformation is a tub structure with D_{2d} symmetry. It has three π^* antibonding orbitals ($3a_2$, $8e$, and $4b_1$) to which promotion of C $1s$ electrons may occur. The orbital ordering is thought to be $3a_2$, $8e$, and $4b_1$[42] with a 1 to 2 eV separation between the $3a_2$ and $8e$ levels and again between the $8e$ and $4b_1$ levels. Thus features 1, 2, and 3 are assigned to transitions to the $3a_2$, $8e$, and $4b_1$ π^* orbitals, respectively.

B. Solid and monolayer spectra of C_5H_8 and C_8H_8

The NEXAFS spectra of solid and monolayer C_5H_8 and C_8H_8 are shown in Figs. 6 and 7. The energies and peak assignments are listed in Tables IV and V. As with cyclobutane (Fig. 3), cyclohexane (Fig. 4), benzene, and pyridine,[4] and thiophene,[41] the condensed phase and gas phase spectra are generally similar indicating that the features are predominantly intramolecular.

The resonances in the spectrum of multilayer cyclopentene show a much lesser degree of polarization dependence than those of cyclohexane. Analysis of the relative peak intensities yields an orientation factor (as defined in Sec. III D) of 1.2 indicating that the cyclopentene multilayer is essentially randomly oriented. By contrast the spectra of monolayer C_5H_8 is highly polarized, with the normal incidence spectrum showing essentially only the σ^*(C–C) and σ^*(C=C) features (#3, #4). Strong σ^* and weak π^* resonances at normal incidence are consistent with an oriented chemisorbed geometry with the double bond parallel to the metal surface. The glancing incidence monolayer spectrum shows enhancement of both features 1 and 2 and weaker σ^* intensity, consistent with the spectral assignments and the proposed surface geometry. An alternate interpretation of feature 2 is as a transition to a σ^*(C–Pt) level, similar to that identified in di-σ bonded ethylene on Pt(111)[18,43] and also similar to our suggested assignment of feature 2 in the monolayer spectrum of cyclooctatetraene (see below). Avery[47]

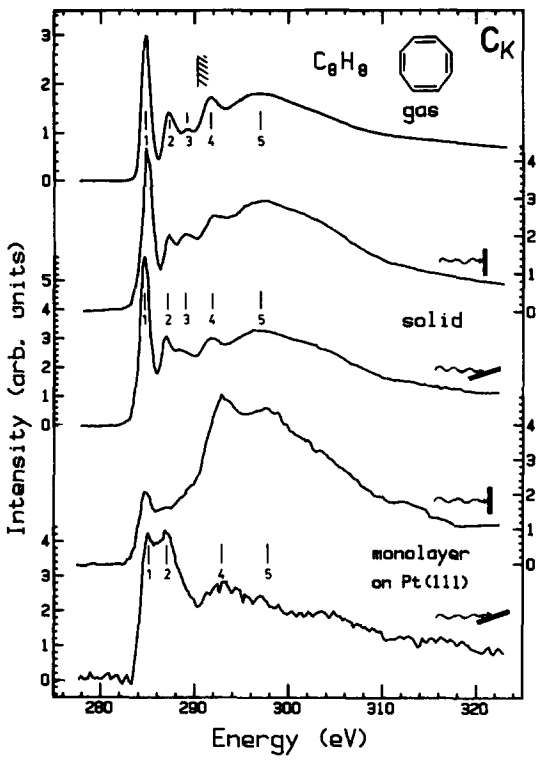

FIG. 7. (a) The carbon *K*-shell ISEEL spectrum of gaseous cyclooctatetratraene. (b) The carbon *K*-carbon normal incidence NEXAFS spectrum of solid (multilayer) cyclooctatetraene condensed at 100 K. (c) The glancing incidence NEXAFS spectrum of solid (multilayer) cyclooctatetraene. (d) The normal incidence NEAFS spectrum of solid (multilayer) cyclooctatetraene on Pt(111) produced by heating the multilayer sample to 210 K. (e) The glancing incidence NEXAFS spectrum of a monolayer of cyclooctatetratraene on Pt(111) (heated to 210 K). The spectra shown have had a background subtracted.

has used vibrational energy loss spectra to deduce an $\eta^2(\mathrm{di}\text{-}\sigma)$ rather than a π donor–acceptor bonding character for *c*-C_5H_8 adsorbed on Pt(111) below 250 K, in agreement with the latter interpretation. The remaining σ^* intensity in the glancing incidence spectrum indicates that the molecule does not lie completely flat on the surface, consistent either with cyclopentene retaining its open envelope structure on the surface or with a tilted geometry, as Avery[47] suggests.

TABLE IV. Absolute energies and proposed assignments of features observed in the carbon *K*-shell spectra of gas, multilayer, and monolayer cyclopentene on Pt(111).

		Multilayer		Monolayer		
Feature	Gas ± 0.1 eV	90° ± 0.5 eV	20°	90° ± 0.5 eV	20°	Assignment final orbital
1	285.0	285.2	285.2	···	284.6	π^* (C=C)
2	287.6	288.4	288.3	···	287.0	π^* (CH_2)
I.P.	290.4[a]					
3	290.6	290.8	290.8	290.6	290.8	σ^* (C–C)
4	295.6	296.0	295.8	295.0	296.3	σ^* (C=C)

[a] Estimated from the I.P.'s of similar hydrocarbons (Ref. 26).

TABLE V. Absolute energies and proposed assignments of features observed in the carbon *K*-shell spectra of gas, multilayer, and monolayer cyclooctatetraene on Pt(111).

		Multilayer		Monolayer		
Feature	Gas ± 0.1 eV	90° ± 0.5 eV	20°	90° ± 0.5 eV	20°	Assignment final orbital
1	284.8[a]	284.9	284.6	284.7	285.0	π^* ($3a_2$)
2	287.3	287.2	287.0	···	286.9[c]	π^* ($8e$)
3	289.3	288.9	288.4	···	···	π^* ($4b_1$)
I.P.	290.3[b]					
4	291.8	291.9	291.8	292.8	292.8	σ^* (C–C)
5	296.9	297.0	296.5	297.5	···	σ^* (C=C)

[a] This feature is located 2.60(9) eV below the π^* transition in CO (Ref. 13).
[b] Estimated from the I.P.'s of similar hydrocarbons (Ref. 26).
[c] In the monolayer contributions from a σ^*(C–Pt) state dominate. See the text for further details.

The NEXAFS spectra of multilayer C_8H_8 (Fig. 7) show distinct differences from the gas phase spectrum in the region of the C $1s \rightarrow \pi^*$ transitions. Whereas feature 3 is weaker than feature 2 in the gas phase spectrum it has greater intensity in the normal incidence multilayer spectrum. Changes in relative intensities of the π^* levels on condensation may be an indication of intermolecular or molecule–surface interactions. The presence of features 2 and 3 in the multilayer spectra of C_8H_8 indicates that they are not Rydberg transitions and supports their proposed assignment to π^* transitions.

Features 4 and 5 dominate the normal incidence monolayer spectrum and are associated with the σ^*(C–C) and σ^*(C=C) shape resonances. The relative intensities of features 1 and 2 in the monolayer spectrum differ considerably from those in the corresponding region of the multilayer or gas phase spectrum. Analysis of the polarization dependence of peak 1[44] shows that the π^* orbitals giving rise to this feature are tilted at 45 ± 3° with respect to the surface normal indicating a symmetric chemisorption geometry in the tub conformation with bonding to the Pt surface at carbons 1, 2, 5, and 6. This places all of the π^* orbitals at the same angle relative to the surface so that in the unperturbed molecule all of the π^* states will have the same polarization dependence. This clearly indicates that peak 2 in the glancing incidence monolayer spectrum is not exclusively π^*(C=C) in origin. It is suggested that this state is associated with transitions to a metal–carbon σ^* level involving rehybridization towards sp^3 of the carbon atoms bound to the surface. The position of feature 2 (287.0 eV) is similar to that of the metal–carbon antibonding sigma level in ethylene on Pt(111) as observed by NEXAFS[43] and supported by MS-$X\alpha$ calculations.[18]

V. RELATIONSHIP BETWEEN σ* RESONANCE POSITION AND BOND LENGTHS

Recently a linear correlation between the position of σ shape resonances and bond lengths has been documented.[2] For carbon–carbon bond lengths this relationship was determined empirically from the inner-shell excitation spectra of primarily *noncyclic* hydrocarbons. In general this linear relationship exists among inner-shell excitation resonances of

molecules in groups where Z, the sum of the atomic numbers of the core-excited atom and its nearest neighbor, are the same. The linear correlation holds best for simple diatomic or pseudodiatomic molecules. Table VI summarizes the shape resonance positions and bond lengths for the molecules examined in this paper. For cyclopropane the position of feature 3 gives best agreement with the previous correlation. However, as with all the other cycloalkanes, the σ^*(C–C) resonance intensity is distributed over several spectral features whereas there is only a single C–C bond length for each molecule. In order to account for this it is appropriate to compare a weighted average of the σ^*(C–C) states to the correlation predictions.[2] An estimated background has been subtracted from each spectrum in order to isolate the σ^* features (as shown in Fig. 8) and the intensity weighted average positions have been computed. These are listed in Table VI. In general there is somewhat better agreement between the position predicted from the bond length and the previous correlation line[2] with the intensity weighted average position than with the position of the most intense σ^*(C–C) resonance.

To illustrate the agreement between the present results and the previously derived relationship,[2] the position of the most intense resonance has been plotted against bond length for each of the species studied in this work (Fig. 9). The solid straight line is a least squares fit to all of the ($Z = 12$) bond length/resonance data available to date (see Refs. 2, 4, and 34 for tabulations of other data used to derive the correlation line) whereas the dashed line is the correlation based on earlier data.[2] The updated correlation parameters in the linear relation

$$\delta = m - nR$$

are $n = -0.468$ eV/pm, $m = 72.5$ eV with a correlation coefficient of -0.94. For carbon–carbon single bonds the agreement between the predicted and observed resonance positions is generally very good for all of the cycloalkanes except cyclopropane. In particular the resonance position increases with decreasing bond length from C_4H_8 to C_6H_{12}.

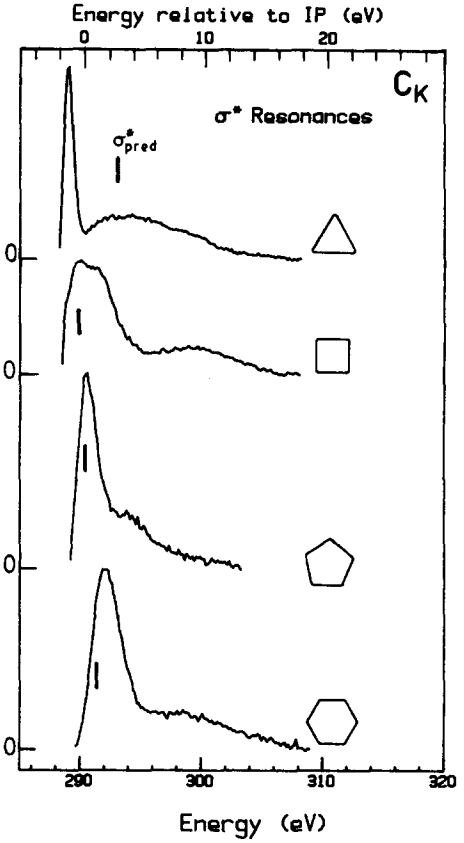

FIG. 8. The carbon 1*s* spectra of the cycloalkanes in the regions of the σ^* resonances after subtraction of an estimated background corresponding to the nonresonant C 1*s* continuum. The lines indicate the σ^* resonance positions predicted by the $Z = 12$ bond length correlation line.

According to the correlation the shorter C–C bond length of cyclopropane should result in a shift of the σ^*(C–C) resonance to higher energy. However the most intense a_2' resonance is about 4 eV below the predicted position (see Fig. 8). The intensity weighted average position for cyclopropane is in reasonable agreement with the correlation. The break-

TABLE VI. Sigma shape resonance position relative to the I.P. of gas phase cyclic hydrocarbons: C_3H_6, C_4H_8, C_5H_8, C_5H_{10}, C_6H_{10}, C_6H_{12}, and C_8H_8.

				δ (eV)[b]					
		Bond lengths (pm)[a]		Pred.		Obs.		Average	
Molecule	I.P.[c]	C–C	C=C	C–C	C=C	C–C	C=C	Pred.[d]	Obs.[e]
C_3H_6	290.6	151.1(3)	···	2.5		2.6	···	2.5	3.1
C_4H_8	290.5	155.6(3)	···	0.0		−0.6	···	0.0	3.0
C_5H_{10}	290.4	154.6(2)	···	0.6		0.1	···	0.6	2.4
C_6H_{12}	290.3	153.5(2)	···	1.1		1.6	···	1.1	4.8
C_5H_8	290.3	152.9(2)	135(2)	1.5	11.2	0.3	5.3	3.4	5.2
C_6H_{10}	290.3	152. (2)	134(2)	2.0	11.8	1.7	8.2	3.6	6.2
C_8H_8	290.3	147.6(3)	134(2)	4.4	11.8	1.5	6.6	8.1	7.3

[a] From microwave or electron diffraction (Ref. 27). The double bond lengths of the alkenes are estimated.
[b] $\delta = E -$ I.P. The predicted values were derived using the least squares correlation parameters for $Z = 12$ given previously (Ref. 2): $\delta = m - n^*R$ where $m = 84.73$ and $n = 0.545$ eV pm^{-1}.
[c] Measured by XPS (Ref. 26) or estimated from the I.P.'s of similar species.
[d] The predicted position for the cycloalkenes is a number weighted average of the C–C and C=C bond lengths.
[e] This entry is the intensity weighted average of all σ^* intensity after background subtraction (see Fig. 8).

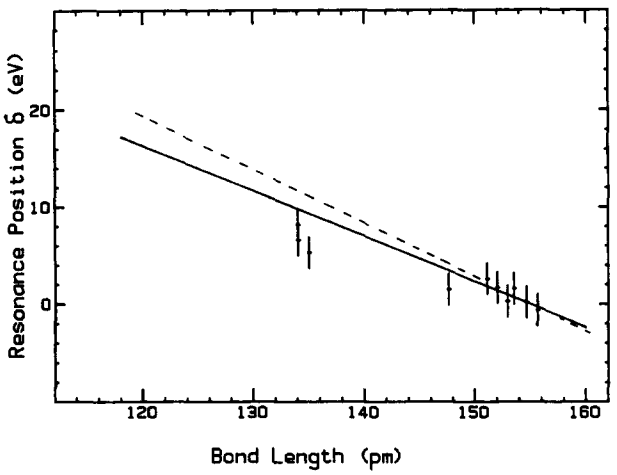

FIG. 9. The position of gas phase σ shape resonances relative to the C *K*-shell I.P. vs carbon–carbon bond distance for a range of organic compounds. The solid line is a linear least squares fit to all carbon *K*-shell resonance data available, while the dashed line is the ($Z = 12$) correlation line reported previously (see the text for references).

down of the simple one-bond/one-resonance picture in cyclopropane (and to some extent in cyclobutane, where the σ^* intensity is also widely dispersed) may be interpreted as an effect of the strained geometry of the smallest carbocyclic rings. This results in in-ring and out-of-ring σ^* orbitals which make large angles with respect to the internuclear C–C axis (cf. schemes 1 and 2).

The agreement between the best fit line and the position of the higher energy σ^*(C=C) resonances is significantly poorer for the cycloalkenes. This is also the trend observed in our earlier work[2] indicating that the simple linear correlation is less accurate in describing double than single bond σ^* resonances. To some extent this may reflect the greater uncertainty in determining the peak location for the broader resonances at higher energy in the continuum. In addition the present work and related studies of saturated heterocyclics[34] and noncyclic alkanes[35] indicate that additional σ^*(C–C) states associated with the saturated regions of the alkenes will occur in the same region as the σ^*(C=C) resonance. This is probably why there is improved agreement between the intensity weighted average of both the σ^*(C–C) and σ^*(C=C) experimental features and the position predicted by the correlation based on the weighted average carbon carbon bond length (Table VI). The presence of σ^* resonances attributed to both the saturated and unsaturated regions of olefins suggests that mixing will occur. This raises the question as to whether it is meaningful even to discuss separate σ^*(C–C) and σ^*(C=C) states in these types of molecules. Although mixing will occur, the dramatic changes in the relative intensities of the C–C and C=C resonance regions which are consistent with the changes in molecular structure (Fig. 5) is direct evidence that it is meaningful to divide the σ^* intensity into regions predominantly associated with either the single or double bonds.

The present results suggest that ring strain plays a role in determining the observed continuum resonance structure. In particular, among the cycloalkanes the higher energy σ^* state is observed more strongly in the smaller rings (see Fig. 1). This trend was also noted in studies of heterocyclics[34] and noncyclic alkanes.[35] The present results indicate that although the empirical relationship can give reasonable, and in some cases quite accurate estimates of bond length, there are factors other than bond length which influence the appearance of the core ionization continuum and the position of σ^* continuum resonances.

In order to directly measure the relationship between σ^* resonance position and bond length for condensed phases the reference level, the ionization threshold relative to E_F, must be known. Unfortunately condensed phase I.P.s are only available for cyclobutane and cyclohexane.[37] We do note that the σ^* resonance positions of all of the molecules are the same within a few eV in the condensed and gas phase spectra (see Tables II, IV, and V) which suggests that the structures of the molecules in the surface and solid phases studied are similar to their gas phase structures.

VI. CONCLUSIONS

The C 1*s* spectra of gas phase C_3H_6, C_5H_{10}, and C_6H_{10}; the C 1*s* spectra of gas and solid C_4H_8; and the C 1*s* spectra of gas, solid, and monolayer C_5H_8, C_6H_{12}, and C_8H_8 have been recorded at moderate resolution and all features assigned. To our knowledge the spectra of these molecules have not been recorded previously. The spectra are dominated by π^* and σ^* intramolecular shape resonances. Except for cyclopropane the correlation between bond length and the position of the main σ^* shape resonance is in reasonable agreement with that reported earlier.[2] The polarization dependence of the monolayer spectra and the absence of shifts in the continuum resonance positions provided information about the chemisorption geometry and orientation. Based on the deduced orientations the observed polarization dependence is consistent with our assignments for all features.

ACKNOWLEDGMENTS

Allen L. Johnson wishes to acknowledge the support of the National Science Foundation and the Chemical Sciences Division of the Department of Energy under Contract No. DE-AC03-76SF00098. The condensed phase studies were done at the Stanford Synchrotron Radiation Laboratory which is supported by the Office of Basic Energy Sciences of DOE and the Division of Materials Research of NSF. The gas phase studies at McMaster were supported by grants from the Natural Sciences and Engineering Research Council of Canada (NSERC). A. P. Hitchcock acknowledges the support of an NSERC University Research Fellowship.

[1] C. E. Brion, S. Daviel, R. N. S. Sodhi, and A. P. Hitchcock, AIP Conference Proceedings **94**, 426 (1982); A. P. Hitchcock, J. Electron Spectrosc. Relat. Phenom. **25**, 245 (1982).
[2] F. Sette, J. Stöhr, and A. P. Hitchcock, J. Chem. Phys. **81**, 4906 (1984).
[3] J. Stöhr and R. Jaeger, Phys. Rev. B **2**, 4111 (1982).
[4] J. A. Horsley, J. Stöhr, A. P. Hitchcock, D. C. Newbury, A. L. Johnson, and F. Sette, J. Chem. Phys. **83**, 6099 (1985).
[5] A. L. Johnson, E. L. Muetterties, and J. Stöhr, J. Am. Chem. Soc. **105**, 7183 (1983).

[6]R. S. Mulliken, Acc. Chem. Res. **9**, 7 (1976); Chem. Phys. Lett. **46**, 197 (1977).
[7]R. A. Rosenberg, P. R. Laroe, V. Rehn, J. Stöhr, R. Jaeger, and C. C. Parks, Phys. Rev. B **28**, 3026 (1983); R. A. Rosenberg, P. J. Love, P. R. Laroe, V. Rehn, and C. C. Parks, *ibid.* **31**, 2634 (1985).
[8]R. Jaeger, J. Stöhr, and T. Kendelewicz, Surf. Sci. **134**, 547 (1983).
[9]J. Stöhr (unpublished results).
[10]G. R. Wight and C. E. Brion, J. Electron Spectrosc. Relat. Phenom. **4**, 25 (1974).
[11]D. E. Ramaker, Chem. Phys. **80**, 183 (1983).
[12]A. P. Hitchcock, S. Beaulieu, T. Steel, J. Stöhr, and F. Sette, J. Chem. Phys. **80**, 3927 (1984).
[13]R. N. S. Sodhi and C. E. Brion, J. Electron Spectrosc. Relat. Phenom. **34**, 363 (1984).
[14]G. R. Wight and C. E. Brion, J. Electron Spectrosc. Relat. Phenom. **3**, 191 (1974).
[15]A. P. Hitchcock and C. E. Brion, J. Electron Specrosc. Relat. Phenom. **10**, 317 (1977).
[16]J. Stöhr, in *Chemistry and Physics of Solid Surfaces*, edited by R. Vaneslow and R. Howe (Springer, Berlin, 1984), Vol. V, p. 231.
[17]K. H. Johnson, Adv. Quantum Chem. **7**, 143 (1973).
[18]J. A. Horsley, J. Stöhr, and R. J. Koestner, J. Chem. Phys. **83**, 3146 (1985).
[19]O. Bastiansen, F. N. Fritsch, and K. Hedberg, Acta Crystallogr. **17**, 538 (1964).
[20]A. Almenningen and O. Bastiansen, Acta Chem. Scand. **15**, 711 (1961).
[21]T. Ueda and T. Shimanouchi, J. Chem. Phys. **47**, 333 (1967); **49**, 470 (1968).
[22]S. Meiboom and L. C. Snyder, J. Chem. Phys. **52**, 3857 (1970).
[23]J. W. Davenport, Phys. Rev. Lett. **36**, 945 (1976).
[24]L. Noodleman, J. Chem. Phys. **64**, 2343 (1976).
[25]J. L. Dehmer and D. Dill, J. Chem. Phys. **65**, 5327 (1976).
[26]A. A. Bakke, H. W. Chen, and W. J. Jolly, J. Electron Spectrosc. Relat. Phenom. **20**, 333 (1980); K. D. Bomben, C. J. Eyermann, and W. L. Jolly, (Jan. 1986) updated list of XPS IP's.
[27]*Landolt–Bornstein, Structure Data of Free Polyatomic Molecules*, (Springer, Berlin, 1976), New Series II, Vol. 7.
[28]L. Jorgensen and L. Salem, *The Organic Chemists Book of Orbitals* (Academic, New York, 1973).
[29]R. Hoffmann and R. B. Davidson, J. Am. Chem. Soc. **93** 5699 (1971).
[30]H. Basch, M. B. Robin, N. A. Keubler, C. Baker, and D. W. Turner, J. Chem. Phys. **51**, 52 (1969).
[31]R. J. Buenker and S. D. Peyerimhoff, J. Phys. Chem. **73**, 1299 (1969).
[32]M. B. Robin, Chem. Phys. Lett. **119**, 33 (1985).
[33]J. P. Doering, A. Gedanken, A. P. Hitchcock, P. Fischer, J. Moore, J. K. Olthoff, J. Tossell, K. Ragavachari, and M. B. Robin, J. Am. Chem. Soc. **108**, 3602 (1986).
[34]D. C. Newbury, I. Ishii, and A. P. Hitchcock, Can. J. Chem. **64**, 1145 (1986).
[35]A. P. Hitchcock and I. Ishii, J. Electron Spectrosc. Relat. Phenom. (in press).
[36]M. B. Robin, *Higher Excited States of Polyatomic Molecules* (Academic, New York, 1974), Vol. 1.
[37]R. J. Koestner (private communication).
[38]A. P. Hitchcock, M. Pocock, and C. E. Brion, Chem. Phys. Lett. **49**, 1259 (1977).
[39]J. A. Horsley and F. Flouquet, Chem. Phys. Lett. **5**, 165 (1970).
[40]D. Arvantis, U. Döbler, L. Wenzel, K. Baberschke, and J. Stöhr, Surf. Sci. (in press).
[41]A. P. Hitchcock, J. A. Horsley, and J. Stöhr, J. Chem. Phys. **85**, 4835 (1986).
[42]P. Frueholz and A. Kuppermann, J. Chem. Phys. **69**, 3614 (1978).
[43]R. J. Koestner, J. Stöhr, J. L. Gland, and J. A. Horsley, Chem. Phys. Lett. **105**, 332 (1984).
[44]A. L. Johnson, V. Grassian, E. L. Muetterties, J. Stöhr, and F. Sette (in preparation).
[45]U. Gelius, P. F. Heden, J. Hedman, B. J. Lindberg, R. Manne, C. Nordling, and K. Siegbahn, Phys. Scr. **2**, 70 (1970).
[46]C. Fridh, J. Chem. Soc. Faraday Trans. 2 **75**, 993 (1979).
[47]N. Avery, Surf. Sci. **146**, 363 (1984).